# THERMAL DYNAMICS OF NONVICINAL METAL SURFACES

Klaus Kern

Institut für Grenzflächenforschung und Vakuumphysik
Forschungszentrum Jülich, Postfach 1913, D-5170 Jülich, FRG

## 1. INTRODUCTION

The atoms in the surface of a crystal are missing part of their nearest neighbors which gives rise to a charge redistribution in the selvedge. This changed force field is responsible for noticeable interlayer relaxations in the near surface region. Intuitively the inward relaxation of the outermost surface layer can be explained by the tendency of the valence electrons to spill over the surface in order to create a lateral smoothing of the electronic charge density[1]. The new electron distribution causes electrostatic forces on the ion cores of the surface atoms, resulting in a contraction of the first interlayer spacing ($d_{12} < d_b$). This relaxation is most pronounced for open, loosely packed, surfaces. In addition, the changes in the force field can also favor lateral atomic rearrangements in the surface plane. The surface "reconstructs" into a phase with new symmetry. These reconstructive surface phase transition can either occur spontaneously or be activated by temperature or by small amounts of adsorbates [2].

So far we have neglected the temperature of the system. As the temperature rises, however, the lattice vibrational amplitude increases and the anharmonic terms in the interaction potential gain importance. Due to the reduced number of nearest neighbors in the surface (a maximum of 9 at the surface of a fcc-crystal with respect to the 12 nearest neighbors in the bulk of this crystal) the mean-square amplitude of the surface atoms is much larger than in the bulk. While in bulk Cu, for example, anharmonicity is negligible below 70-80% of the melting temperature, anharmonicity on the Cu(110) surface becomes important at temperatures above 40% of the melting

*Phase Transitions in Surface Films 2*
Edited by H. Taub *et al.*, Plenum Press, New York, 1991

temperature (the bulk Debye temperature of copper is $\Theta_B$ = 343 K, and the melting temperature is $T_M$ = 1356 K).

At the high temperature end it has been demonstrated recently that on a variety of surfaces a disordered quasi-liquid layer wets the surface well below the bulk melting temperature, i.e. the melting of a crystal starts from the surface layer [3]. In view of the Lindemann criterion of melting [4], which states that melting occurs when the mean-square displacement of the atoms surpasses a critical value (~ 10% of the interatomic equilibrium distance), the important role that surfaces play in the melting phase transition is not surprising. As already discussed the mean vibrational amplitude is substantially enhanced at the surface and the Lindemann-criterion predicts a surface instability around 0.75 $T_M$.

The picture developed above is based on a perfect defect free surface, which is, however, only at zero temperature the stable equilibrium state. At elevated temperatures a certain amount of defects like isolated adatoms and vacancies as well as clusters of those can be thermally excited. Both adatom islands as well as vacancy holes are bordered by steps. Frenkel [5] studied the structure of such steps and argued that they should contain a large number of kinks at finite temperatures. Thus due to thermal fluctuations every crystal surface with steps, should have a certain microscopic roughness at nonzero temperature, the surface remains flat on macroscopic length scales however. Burton and coworkers, demonstrated that the thermal excitation of adatom and vacancy islands and thus the excitation of steps is negligible at low and medium temperatures but gave evidence for the presence of a roughening transition, at a temperature close to the bulk melting temperature, where the surface becomes macroscopically rough[6,7]. The critical temperature of this transition has been termed the roughening temperature, $T_R$. Burton et al. suggested that at the roughening temperature the free energy associated with the creation of a step vanishes. This was confirmed later by Swendsen in a detailed calculation [8]. One of the fundamental consequences of the existence of a roughening temperature for a certain crystallographic face below the melting temperature is that this face can occur on an equilibrium crystal only at temperatures below $T_R$.

Let us consider a surface which at T = 0 K is perfectly flat. Upon increasing the temperature, thermal fluctuations give rise to vacancies, adatoms atoms and steps in the surface layer. The number of these "defects"

increases until, at the roughening temperature, the long-range order of the surface disappeares. Long-range order is confined here to the "height-correlation function" and not to the positional correlation function (parallel to the surface plane). Indeed, even above the roughening temperature, the surface atoms populate in average regular lattice sites. It is the fluctuation of the height h(r) which diverges for temperatures T $> T_R$ [9].

$$\langle[(h(\vec{r}') + \vec{r}) - h(\vec{r})]^2\rangle \propto C(T)\ln(\vec{r}) \qquad (1)$$

where C is a temperature-dependent constant and $\vec{r}$ a two-dimensional vector in a plane parallel to the surface. This divergence is very weak. At the roughening temperature $C(T_R) = 2/\pi^2$; the height fluctuation is one lattice spacing for a distance of 139 lattice spacings.

The first direct experimental evidence for a roughening transition was reported in 1979. Several groups have studied the thermal behavior of the basal plane of a hexagonal close-packed $^4$He crystal [10]. In a beautiful experiment Balibar and Casting obtained for this surface a roughening temperature of $T_R \approx 1.2$ K.

More recently, the question of thermal roughening has also been addressed in the study of metal surfaces. Detailed He diffraction studies from the high Miller index (11n) with n=3,5,7 surfaces of Cu [11] and Ni [12] proved the existence of a roughening transition on these surface.

The microscopic mechanism which leads to the roughening of a low and a high Miller index surface is expected to be different. Indeed, as already mentioned, a low indexed surface - which at T = 0 K is perfectly flat - fulfills the roughening condition, Eq. (1), when the free energy for the creation of a step becomes zero. In contrast, on a high indexed surface - which at T = 0 K is already stepped - Eq. (1) can be fulfilled also without the creation of new steps. It appears that the proliferation of kinks is sufficient to roughen the vicinal surface. Indeed, the ensuing meandering of the step rows, in conjunction with the mutual repulsion between these rows, leads also to the divergence of the "height-correlation function". Thus, the roughening temperature of high indexed surfaces is substantially lower than that of the low indexed ones. In the case of Cu and Ni(11n) the values for $T_R$ range from 300 K to 720 K (Cu) and 450-750 K (Ni) for n = 3,5,7.

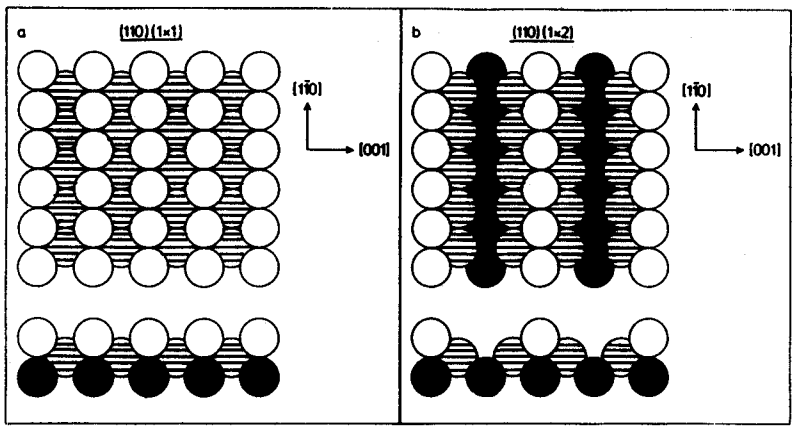


Fig. 1. Structure of the unreconstructed and reconstructed (110) surface of face centered cubic metals.

While the existence of a roughening transition on stepped vicinal surfaces is undisputed, the basic question whether $T_R$ of low indexed surfaces is lower than the crystal melting temperature $T_M$ or not is still matter of controversial discussion. The magnitude of $T_R$ is governed by the bond strength at the surface. Thus, close packed surfaces with more neighbors and stronger bonds have a higher roughening temperature than more open surfaces.

Particularly attractive for roughening studies of low index metal surfaces are (110) surfaces of fcc-crystals. Firstly, the (110) surface has the most open structure of the three densest fcc-faces, (111), (100) and (110); resembling to some extent the topography of the (113) surface. The second aspect is surface reconstruction. The (110) surfaces of transition metals with face centered cubic (fcc) symmetry belong to two different classes. The first class, including the 3d-elements Cu, Ni and the 4d-elements Rh, Pd and Ag, have a nonreconstructed (1x1) ground state for the clean surface, i.e. they keep the bulk termination (they exhibit however large oscillatory interlayer-relaxations). The second class of fcc metals, including the 5d-elements Ir, Pt and Au, exhibits a reconstructed (1x2) ground state. The nature of the (1x2) reconstruction has been studied extensively by a number of different experimental techniques and there is a general agreement now that the (1x2) phase of all three 5d-metals is a missing row geometry [13] with every second close packed [1$\bar{1}$0] row missing (see fig. 1).

It was suggested that reconstruction and roughening in these systems are indeed related /14/. As pointed out by Garofalo et al. the energies of the relaxed unreconstructed (1x1) surface and the energies for all possible missing-row states (1x2, 1x3, ...,1x4), are all energetically close to one another [15]. Locally the (1xn) reconstructions represent microscopic (111) facets and are expected to be easily excitable at elevated temperatures. Trayanov et al. [14] speculate, that whatever the low-temperature ground state configuration (unreconstructed or reconstructed) it might roughen into a high temperature disordered phase, with a mixture of (1xn) configurations.

## 2. DETECTION OF STEPS

Very attractive techniques to detect monatomic steps on surfaces are direct imaging methods such as scanning tunneling microscopy (STM). In a typical constant-current topography scan a surface step is easily identified as a vertical movement of the tip by one lattice spacing. The step structure (kinks) and orientation are easily determined. The main drawback of STM in the determination of step densities and distributions is its limited scan range and the narrow temperature range for stable operation (in particular high temperature measurements have not been reported so far).

The classic technqiue for the analysis of defect structures on surfaces is certainly diffraction (LEED, X-ray, He-diffraction). In a first order approximation the diffracted intensity from a perfect single crystal surface drops exponentially with temperature, according to the Debye-Waller formula

$$I \sim \exp(-2W) = \exp[-\langle (Q\cdot u)^2 \rangle] \qquad (2)$$

Thermal excitation of adatoms, vacancies, roughening or lateral disordering but also anharmonicity all give rise to anamalous thermal behavior associated with a more rapid decrease of the diffracted intensity. Thus a simple intensity analysis does not allow to distinguish between these channels.

Step proliferation (i.e. roughening) however can be unambigously detected in a diffraction experiment by the width or line-shape analysis of the diffraction peak under well defined kinematical conditions. To

illustrate that we consider a plane wave which is scattered from two adjacent terraces separated by a monatomic step. Beams diffracted from the upper and the lower terraces will interfere. If the interference is constructive or in-phase (i.e. the phase between the two waves is an even multiple of $\pi$), the diffraction peak is identical to that of the ideal step free surface. For the case of destructive interference or anti-phase diffraction (i.e. the phase between the two waves is an odd multiple of $\pi$), however, all diffraction peaks will be broadened with a maximum halfwidth proportional to the average step density. Thus, in an anti-phase kinematics a diffraction experiment is very sensitive to the presence of steps. At the roughening temperature $T_R$ the anti-phase Bragg-peak is broadened by ~ 60%.

The diffracted intensity which is removed from the peak center is distributed into its wings, i.e. the line shape of the peak changes due to the presence of steps. At the roughening temperature the line shape of the diffraction peak is described by a power law [16]:

$$I(Q_{\parallel}) \propto Q_{\parallel}^{-(2-\tau)} \qquad (3)$$

$Q_{\parallel}$ being the parallel momentum transfer and $\tau$ the so called roughness exponent

$$\tau = \frac{\pi}{2} K(T)\ f(p) \qquad (4)$$

K(T) is the so called roughness parameter. Everywhere in the low temperature phase the effective K(T) is equal to zero (no powerlaw line shape); at the roughening transition it jumps to the universal value $K(T_R) = 2/\pi$ (see e.g. ref. 16), and increases with temperature continuously in the rough phase. The function f(p) describes the scattering kinematics and varies frm f(p)=0 for in-phase diffraction to f(p)=1 in anti-phase geometry. Theoretically f(p) varies with the model and also depends on finite size effects, from a (periodically repeated) square to a simple cosine function of the phase p. Thus, at the roughening temperature in a perfect anti-phase diffraction experiment we have $\tau_R=1$.

In some favorable situations monatomic steps can also give rise to shifted diffraction peaks, and the step density can be extracted directly from the peak shift [17]. Such a case is discussed in chapter 5.

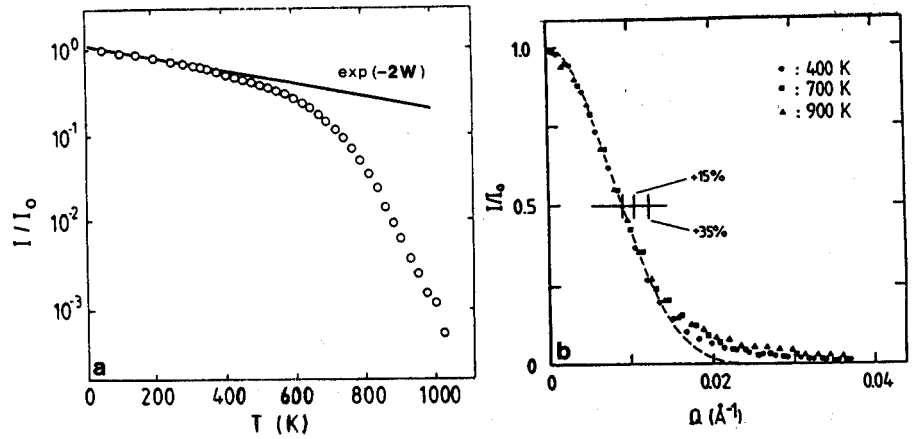


Fig. 2. a) Thermal dependence of the He specular peak height from Cu(110); $E_{He}$ = 18.3 meV, $\vartheta_i = \vartheta_f = 45^o$ [21]. b) Specular He-peak profiles normalized at their maximum (same data as fig. 2 in ref. 21). The verticals bars (+ 15% and + 35%) indicate model based theoretically predicted broadenings at the roughening temperature (square and cosine variation of the phase function f(p) in eq. (4)). The dashed line indicates the gaussian resolution function of the instrument.

## 3. ANHARMONICITY OR ADATOMS

More than ten years ago it had been noticed that the intensities in the photoemission spectra taken from Cu(110) decrease dramatically with temperature above ~ 500 K [18]. Similar effects have been seen recently in low-energy ion scattering [19], in X-ray diffraction [20] and in thermal He scattering [21,22]. The dramatic intensity decrease observed in all cases above 450-500 K could not be accounted for by simple Debye-Waller effects. While Lapujoulade et al. [22] and Fauster et al. [19] proposed as explanation either anharmonic effects or some kind of disorder, Mochrie [20] concluded categorically - without qualitative additional evidence - that he was observing the roughening transition. He even tentatively identified the temperature at which "the intensity has fallen essentially to zero" (870 K) with $T_R$. A He specular intensity measurement on Cu(110) versus temperature performed in our laboratory shows (Fig. 2a) that also above 870 K the intensity continues to drop (at 1000 K it is one order of magnitude lower) and that there is no sign of saturation even above 1000 K. Whether the intensity becomes "essentially zero" appears to depend on the dynamical range of the instrument, and is not a criterion for the choice of value of $T_R$. Zeppenfeld et al. [21] have analyzed in detail the energy and angular distribution of the scattered He atoms in the whole temperature range up to

1000 K. In fig. 2b the specular He-peak profiles taken at three different temperatures are shown. By inspection of this figure it is evident that the strong intensity decay can not be attributed to surface roughening; the specular He-diffraction peak measured in near antiphase-scattering geometry does not show any broadening up to 900 K, clearly demonstrating the abscence of step-proliferation. This is also consistent with the behavior of the diffuse elastically scattered He-intensity which has been found to drop continuously between 100 and 900 K, while at $T_R$ a substantial increase of the diffuse scattering is expected [23].

Lapujoulade and Salanon [24] suggested that the anomalous thermal behavior of the specular He-intensity might be exclusively attributed to the thermal excitation of adatoms and vacancies. In order to explain the He-data quantitatively, however, astronomically high equilibrium defect concentrations would be necessary. With the assumption of a random distribution of adatoms and vacancies the attenuation of the specular He-beam $I/I_0$ is given by $I/I_0 = (1-\Theta)^{n_s \cdot \Sigma}$, here $n_s$ is the number of lattice sites, $\Sigma$ the cross section for diffuse scattering and $\Theta$ the defect concentration. Taking a diffuse He-scattering cross section of 70 $\AA^2$ for a Cu-adatom or vacancy, 3.6% defects would be present already at 500 K increasing to 12% at 700 K and eventually to more than 30% at 900 K. These defect concentrations are without any doubt unreasonable. Using low energy ion scattering Fauster et al. [19] have determined upper limits for the defect concentration of Cu(110); at 500 K the adatom and vacancy density is found to be below 1% and at 800 K it is still below 5%. These values agree with LEED measurements of Cao and Conrad[25] for the homologeous Ni(110) surface, demonstrating that adatom and vacancy creation is negligible below 60% of the melting temperature (0.60 $T_M$ = 813 K for Cu). At temperatures of 0.7 $T_M$ they estimate the defects concentration to range between 5 and 15%. This picture is further supported by recent molecular dynamics calculations for the (110) surfaces of Al, Ni and Cu [26]. These simulations show that the thermal excitation of adatoms and vacancies becomes significant only above ~ 0.7-0.8 $T_M$.

It is generally accepted now that the sharp decrease in coherently scattered intensity above 0.35 $T_M$ is ascribed to an anomalous large increase of the mean-square displacement of the surface atoms $\langle u^2 \rangle$ due to a large anharmonicity in the metal potential at the surface [21,25,27]. This is demonstrated in fig. 3, where the mean square displacement $\langle u^2 \rangle$ at the Cu(110) surface (perpendicular to the surface), as deduced from vastly

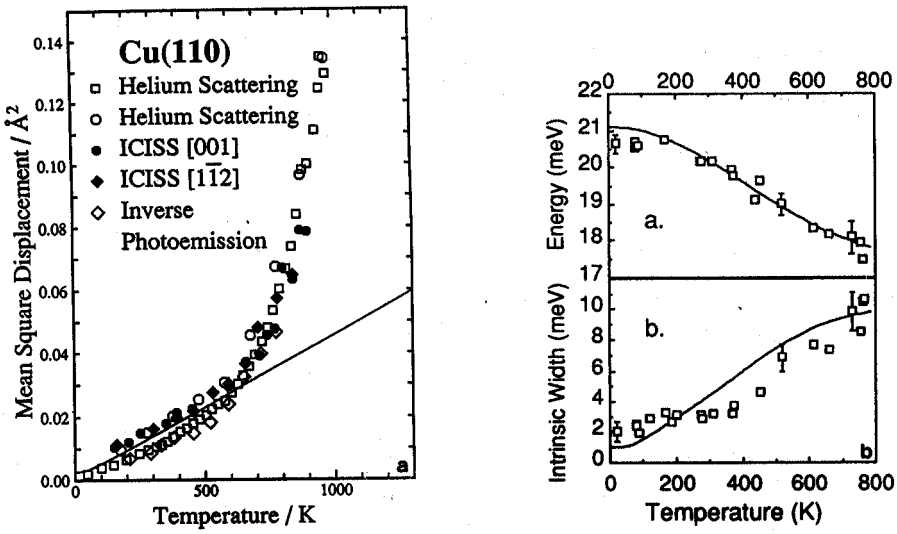


Fig. 3. a) Mean square displacements of surface atoms versus temperature deduced from ion scattering, He-scattering and inverse photoemission [27]. b) Energy and intrinsic width of the Cu(110) $MS_7$ resonance phonon at the $\bar{\Gamma}$-point as a function of temperature[51].

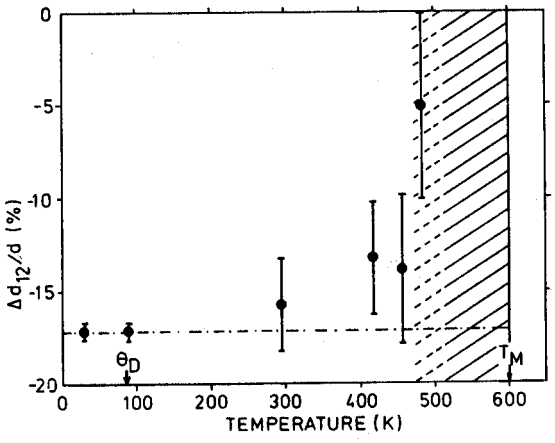


Fig. 4. Surface relaxation of Pb(110) versus temperature [28].

different experimental techniques, is plotted versus temperature. All three techniques agree nicely. A very recent experimental study of the temperature dependent surface phonons has been used to quantify the excess surface anharmonicity of Cu(110)[51]. Above 400 K the $MS_7$ resonance phonon shows a significant decrease of the phonon frequency accompanied by a substantial broadening of its intrinsic width. A simple anharmonic model reproduces the observed temperature effects and a direct comparison with bulk phonons reveal a surface anharmonicity enhanced about 5 times over that of the bulk.

An enhanced surface anharmonicity on the open (110) surface of fcc metal crystals has been deduced also from theoretical as well as experimental studies of the thermal surface expansion coefficient [28,29]. Nonreconstructed fcc(110) surfaces are strongly relaxed and the interlayer distance between the first and second plane of atoms $d_{12}$ is contracted between 5 and 15% with respect to the bulk value $d_b$. This relaxation was found to vanish rapidly above ~ 0.4 $T_M$ (i.e. $d_{12}/d_b \rightarrow 1$) and can only be ascribed to a dramatic increase of the thermal surface expansion coefficient driven by a strong surface anharmonicity. The corresponding experimental graph for Pb(110) [28] is given in fig. 4.

## 4. ROUGHENING OF THE UNRECONSTRUCTED fcc(110) SURFACES

The observation of a surface roughening transition on the (110) faces of Ni and Pb was reported recently by Cao and Conrad [25] and by Yang et al.[34], respectively. Using high resolution LEED these authors showed the onset of step proliferation at ~ 0.75 $T_M$. The roughening transition is preceeded by two stages, a large increase of the mean square displacements of the surface atoms due to excess surface anharmonicity starting at ~ 0.45 $T_M$ followed by adatom and vacancy creation above ~ 0.7 $T_M$.

While in the case of Pb(110) the logarithmic divergence of the height-height correlation function was demonstrated, the roughening of Ni(110) has been deduced from the broadening of the anti-phase Bragg peak.

A detailed analysis of the Ni(110) LEED angular diffraction profiles by Cao and Conrad reveal a Gaussian central peak superimposed on a broad Lorentzian, which is interpreted in a two-level model. In this model the ratio of the Gaussian to the Lorentzian intensity is proportional to the adatom

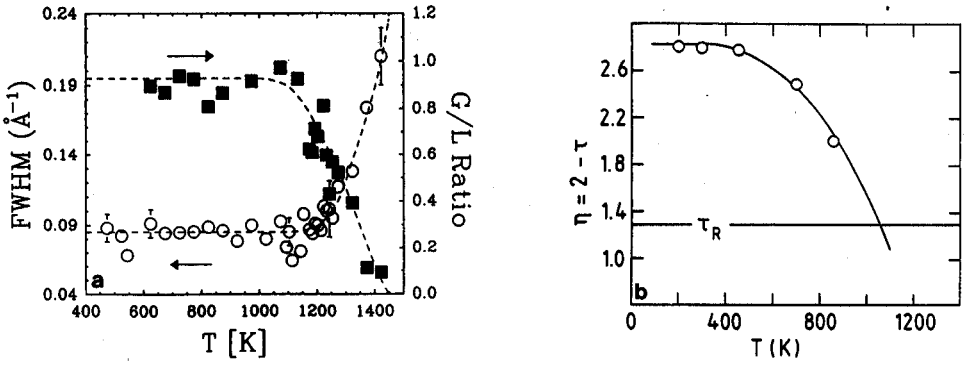


Fig. 5. a) The ratio of the Gaussian to Lorentzian intensity (■) and the Lorentzian FWHM (o) of the specular anti-phase LEED diffraction peak from Ni(110) vs temperature [25]. b) The roughening exponent $\tau$ for Cu(110) obtained from log-log plots of the tail part of the purely elastic specular He-beam.

concentration, the width of the Lorentzian component characterizes the average step density. In Fig. 5a the temperature dependence of these quantities as measured by Cao and Conrad is shown. The onset of adatom creation around 1150 K and the proliferation of steps around 1300 K (= 0.75 $T_M$) are evident. This behavior of the diffraction line-shape may however also be consistent with a preroughening-transition of the type discussed by den Nijs[14,49]. In the preroughening scenario steps are created spontaneously at the transition, but each step up is followed by a step down and vice versa and the surface remains flat on a macroscopic length scale.

From a detailed analysis of the elastic He-diffraction profiles we can estimate that Cu(110) may indeed roughen at similar relativ temperatures (with respect to the bulk melting temperature). In fig. 5b we plot the roughness exponent $\tau$ deduced by Zeppenfeld et al. [21] from log-log plots of the elastic contribution to the polar profiles of the specular peak. At the roughening temperature $\tau_R = 1$ in ideal anti-phase scattering geometry. Correcting for the actual scattering conditions in the experiment of Zeppenfeld et al. gives a roughening exponent $\tau_R = 0.71$ (assuming a cosine-like behavior of the phase factor f(p), which is indeed observed in all thermally roughened surfaces [11,12]). Extrapolating of the data in fig. 5b to this value we can estimate the roughening temperature of Cu(110) to be $T_R \simeq 1070$ K = 0.79 $T_M$.

That this value might indeed be the correct roughening temperature of Cu(110) is supported by diffusion measurements of Bonzel and coworkers. These authors studied the surface self-diffusion of various fcc(110) surfaces by monitoring the decay of a periodic surface profile. The profile with periodicities of a few $\mu$m is prepared by a photoresist masking techniques and subsequent Argon RF-sputtering and the analysis of the profile decay at elevated temperatures is done by laser diffraction [30-32]. The results for Ni(110) and Cu(110) are plotted in fig. 6. Below the roughening temperature the macroscopic diffusion is expected to proceed by single adatom diffusion while above $T_R$ the macroscopic mass transport should be dominated by meandering steps. Surface diffusion of adatoms on the (110) surface of fcc-crystals is expected to be anisotropic because of the twofold symmetry of the surface. This expectation is confirmed by the data in fig. 6. At low temperatures the activation energy for diffusion along the close packed channels, i.e. along the [110] direction, is found to be only 40% of the barrier for across channel diffusion, i.e. diffusion along the [100] azimuth. For Ni as well as Cu(110), however, this anisotropy vanishes at ~ 0.78 $T_M$. Above this temperature the mass transport is isotropic, consistent with two-dimensional step diffusion. We thus conclude that the diffusion data in fig. 6 support a roughening transition of Ni and Cu(110) around 78% of the melting temperature.

Rather unusual evidence for the roughening of Cu(110) around 80% of the melting temperature comes from an optical microscopy study of Freyer [33]. In order to cross-check his diffusion measurements he studied the morphology of sinusoidaly grooved Cu(110) surfaces by means of an interference microscope. The samples were first annealed at high temperatures followed by a rapid quench to room temperature. He always observed a strong morphology change at annealing temperatures between 1050 K and 1100 K; but unfortunately missed the significance of the data. Fig. 7 shows two of his interference micrographs after annealing to 1030 K and 1150 K, respectively, clearly demonstrating the roughening above 1100 K (note that the roughness also appears on the right part of fig. 7b, where the Cu(110) surface is not grooved).

Evidence for the roughening of the (110) surface has also been presented recently for the metals In, Ag and Pd. While the roughening of the In(110) [35] surface is generally accepted the experimental results for Ag(110) [36] and in particular Pd(110) [37] are disputed. For palladium Francis

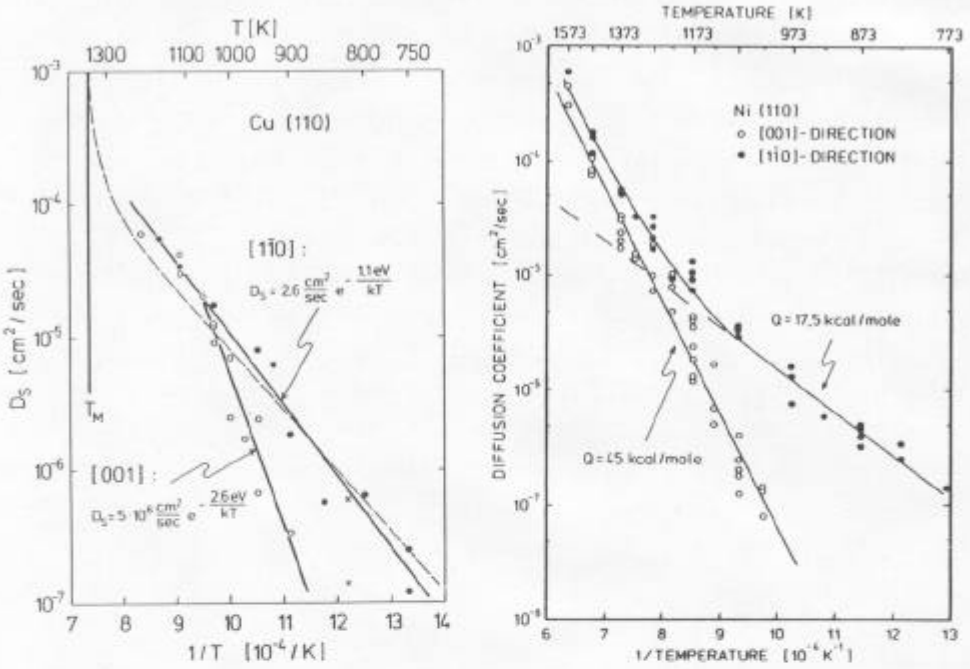


Fig. 6. Arrhenius plot of the surface self-diffusion coefficient for Ni(110) and Cu(110) [30-32]

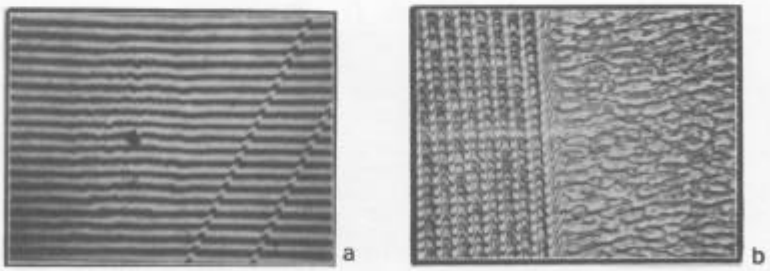


Fig. 7. Optical interference-microscope picture of a grooved Cu(110) surface (average distance between grooves ~ 6μm) upon heating to a) T=1030 K and b) T=1150 K, followed by a rapid quench to room temperature [33].

and Richardson [37] reported an order-disorder transition to occur around 250 K. This transition was, however, not be detected in a series of subsequent experiments [38], and today is believed to be an artifact due to the presence of impurities in the experiments of Francis and Richardson. Ag(110) is an interesting case. This surface was studied by Held et al. with synchrotron x-ray diffraction [36]. Based on a diffraction peak shape analysis they deduced the relatively low roughening temperature of 0.58 $T_M$. This low transition temperature has been connected with the small stabilization energy with respect to the missing row reconstruction [14] but can also be due to a preroughening transition of the type discussed by den Nijs [14]. In addition Robinson [39] suggested recently, that the data analysis might be influenced by the interference with the theraml diffuse scattering of a bulk diffraction peak. The roughening temperatures of nonreconstructed fcc(110) surfaces are summarized in table I.

Table 1. The roughening temperatures of fcc(110)(1x1) metal surfaces

| Surface | $T_R$ [K] | $T_R/T_M$ | References |
|---|---|---|---|
| Ag(110) | 720 | 0.58 | 36 |
| In(110) | 290 | 0.69 | 35 |
| Pb(110) | 420 | 0.70 | 34 |
| Ni(110) | 1300 | 0.76 | 25 |
| Cu(110) | 1070 | 0.79 | 21,32,33 |

## 5. DECONSTRUCTION OF THE RECONSTRUCTED fcc(110)(1x2) SURFACES

In the case of Au(110), the missing row (1x2) phase has been found to be stable only in a limited temperature range. Upon heating, the half order superlattice LEED-spot was seen to change shape with temperature and eventually disappeared at a critical temperature $T_C \simeq 0.49\ T_M \simeq 650$ K, indicating a continuous phase transition from an ordered (1x2) state into a disordered (1x1) phase [40]. Campuzano et al. have analyzed this phase transition in terms of a two dimensional order-disorder transition and determined critical exponents consistent with the predictions of the 2D-Ising model, which, due to the p2mm symmetry of the Au(110)(1x2) surface, is indeed the appropriate universality class [41].

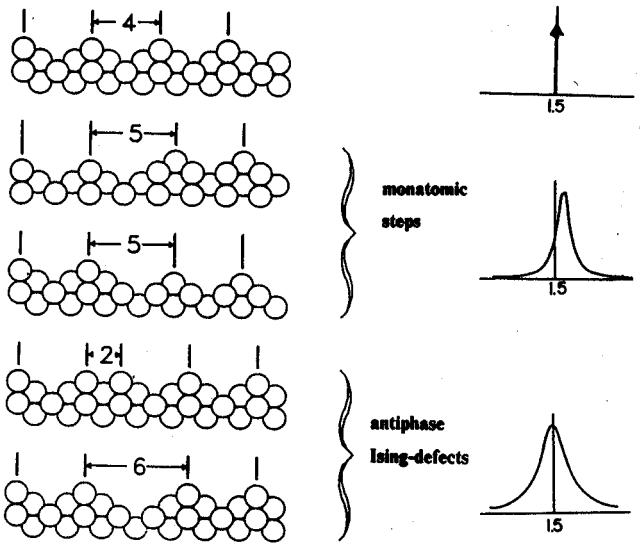


Fig. 8. Thermal excitations of the fcc(110)(1x2) missing tow reconstructed surface; Ising-like antiphase defects and monatomic steps, i.e. (111) micro facets. Also shown schematically is the profile of the half-order diffraction peak with and without defects.

A considerable amount of disorder, however, has also been observed to be present in the low temperature missing row phase of all three metals Ir, Pt and Au [13,42]. While the coherence along the [110]direction (parallel to the close packed rows) extends over several hundred Å,the coherence length along the [001] direction (perpendicular to the rows) hardly surpassed 100-200Å. Scanning tunneling microscopy [42] assigned this intrinsic disorder to the presence of some (1x3) and (1x4) reconstructed regions, which are induced by a micro (111) facetting. In theoretical studies it has been shown that the (1x2) missing row configuration is indeed only marginally stable with respect to the "higher" missing row states (1x3, 1x4, ..., 1xn). The energy difference between any of the (1xn) phases of Au(110) has been calculated to be less than 10meV per atom [15]. Based on this ground it has been argued by several authors that the missing row configuration should be thermally unstable with respect to the formation of (111) microfacets, giving rise to a "rough" surface at elevated temperatures. While Villain and Vilfan [43] have predicted a succesion of two transitions, an Ising-like order-disorder transition at ~ 0.50 $T_M$ (spontaneous proliferation of antiphase Ising-defects, fig. 8) followed by roughening transition at ~ 0.57 $T_M$ (onset of (111) micro facetting generating single height steps, fig. 8), Levi and Touzani [44] have found no evidence for an Ising-like transition but predicted a direct roughening transition.

In a recent x-ray diffraction experiment Robinson, Vlieg and Kern have studied the thermal behavior of the reconstructed Pt(110) surface [45,46]. The experimentally observed half order diffraction peaks have two characteristics: they are broad in the [001] direction but sharp in the orthogonal [1$\bar{1}$0] direction and always displaced slightly from the exact half order position along [001]. The uniaxial broadening and shift implies disorder in one direction only, i.e. must be associated with line defects oriented perpendicular to the [001] direction. An identical pattern of uniaxially shifted and broadened half order diffraction peaks was observed earlier by Robinson et al. [17] for the Au(110) surface and can be explained

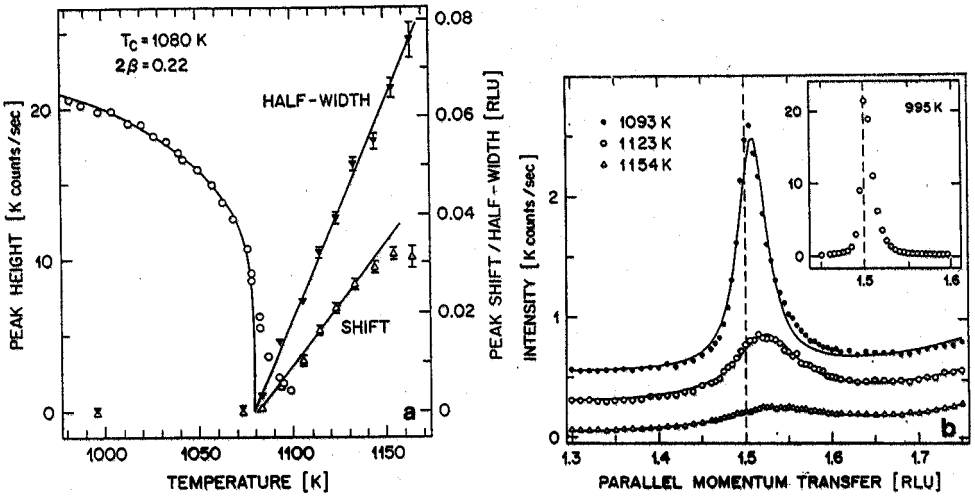


Fig. 9. a) Temperature dependence of the halforder diffraction peak (h, 0.06,0.06) obtained by scanning h [45,46]. b) Temperature dependence of the extracted peak height, width and shift [45,46].

conclusively in terms of randomly distributed single height steps on the surface. It was further demonstrated that the peak shift of the half order spots is exclusively related to the density of these monatomic steps [17,45], while Ising-like defects would only result in a symmetric peak broadening. Indeed, (111) micro facets are also the predominant defects seen in scanning tunneling microscopy images of Au(110) and Pt(110) [42,47].

The temperature dependence of the half-order diffraction profile was measured and found to be have reversibly. The data are summarized in fig. 9, cleary demonstrating a phase transition at a critical temperature of $T_C = 0.53\ T_M = 1080 \pm 1$ K. The peak height, I(T), is fully compatible with a

theoretical curve $I(T) = I_0|t|^{2\beta'}$ where $t=T/T_c-1$ and $\beta' = 0.11 \pm 0.01$. Above $T_c$ the half-width diverges linearly with the reduced temperature. Both of these aspects are exactly in accord with the predictions of the 2D-Ising model, which has $\beta' = 1/8$ and $\nu = 1$ (correlation length exponent), and agree well with the LEED data for the analogous phase transition of Au(110)(1x2).

Notwithstanding this apparent agreement between Pt(110), Au(110) and the 2D Ising model, we now turn to the behavior of the diffraction peak shift in fig. 9b. Above $T_c$ the peak shifts substantially and completely reversibly. This result is in contrast to the Ising classification because it implies that an equilibrium density of steps appears spontaneously above $T_c$. This immediately implicates some roughening character. The slopes of the half-width and peak shift versus T in fig. 9b allow us to quantifiy the line defect density in units of probability per lattice site for the monatomic steps $\alpha = 6.6t$ and antiphase Ising defects $\beta = 2.8\ t$; i.e. thermally induced steps are 2-3 times more common.

Two solutions have been proposed to escape from this paradox. Villain and Vilfan [48] suggest that the steps formed above the transition are bound together in pairs. The imposition of paired steps leads necessarily to a phase transition model in the Ising-universality class due to the twofold degenerated ground state. This model forbids any height divergence and the surface is never rough. Villain and Vilfan suggest a step pair unbinding transition at higher temperatures $T_{c'}>T_c$ which eventually roughens the surface. den Nijs [49], however, suggests a transition with real roughening character but Ising-criticality. In the framework of a 4-states chiral clock step model, den Nijs demonstrated that for negligible chirality the reconstructed (1x2)(110) surface deconstructs and roughens in one single transition which is characterized by Ising exponents. This transition has the character of an incommensurate melting transition with respect to the reconstruction degrees of freedom, explaining the peak shift and the linear vanishing of it at $T_c$. Zero chirality, however, requires that step defects with a phase shift of 3 half-cells (see fig. 8) have also to be present on the surface, but are rarely observed [42] and are expected to be energetically unfavorable [50].

What is needed now is another experiment to test these predictions. It should be possible to measure the temperature dependence of the integer order diffraction peak profiles which are sensitive to roughness. While in

the Villain and Vilfan model no change should be seen; the roughening scenario of den Nijs would result in a significant peak broadening.

REFERENCES


1. M.W. Finnis and V.J. Heine; J. Phys. F4, L37 (1974)
2. J.E. Englesfield; Prog. Surf. Sci. 20, 105 (1985)
3. J.F. van der Veen, B. Pluis, and A.W. Denier van der Gon; in "Physics and Chemistry at Solid Surfaces VII", (Springer, Berlin, 1988), p. 455
4. F.A. Lindemann; Z. Phys. 14, 609 (1910)
5. J. Frenkel; J. Phys. USSR 9, 392 (1945)
6. W.K. Burton and N. Cabrera; Disc. Faraday. Soc. 5, 33 (1949)
7. W.K. Burton, N. Cabrera and F.C. Frank; Philos. Trans. Roy. Soc. London 243 A, 299 (1951)
8. R.W. Swendson; Phys. Rev. B17, 3710 (1978)
9. H. van Beijeren and I. Nolden; in Structure and Dynamics of Surfaces II, (Springer, Berlin, 1986), p. 259; and references therein
10. S. Balibar and B. Castaing; Surf. Sci. Rep. 5, 87 (1985)
11. F. Fabre, D. Gorse, B. Salanon, and J. Lapujoulade; J. Physique 48, 1017 (1987)
12. E.H. Conrad, L.R. Allen, D.L. Blanchard, T. Engel; Surf. Sci. 187, 265 (1987)
13. P. Fery, W. Moritz, D. Wolf; Phys. Rev. B38, 7275 (1988)
14. A. Trayanov, A.C. Levi, and E. Tosatti; Europhys. Lett. 8, 657 (1989); M. den Nijs; Phys. Rev. Lett. 64, 435 (1990)
15. M. Garofalo, E. Tosatti, and F. Ercolessi; Surf. Sci. 188, 321 (1987)
16. J.D. Weeks, in Ordering in Strongly Fluctuating Condensed Matter Systems, Ed. T. Riste, (Plenum, New York, 1980) p. 293
    J. Villain, D.R. Grempel, and J. Lapujoulade; J. Phys. F 15, 809 (1985)
17. I.K. Robinson, Y. Kuk and L.C. Feldman; Phys. Rev. B29, 4762 (1984)
18. R.S. Williams, P.S. Wehner, J. Stöhr and D.A. Shirley; Phys. Rev. Lett. 39, 302 (1977)
19. Th. Fauster, R. Schneider, H. Dürr, G. Engelmann, and E. Taglauer, Surf. Sci. 189/190, 610 (1987)
20. S.G.J. Mochrie; Phys. Rev. Lett. 62, 63 (1987)
21. P. Zeppenfeld, K. Kern, R. David, and G. Comsa; Phys. Rev. Lett. 62,63 (1989)
22. J. Lapujoulade, J. Perreau and A. Kara; Surf. Sci. 129, 59 (1983)
23. E.H. Conrad, L.R. Allen, D.L. Blachard, and T. Engel; Surf. Sci. 198,207 (1988)
24. J. Lapujoulade and B. Salanon, this proceeding
25. Y. Cao and E.H. Conrad; Phys. Rev. Lett. 64, 447 (1990)
26. E.T. Chen, R.N. Barnett and U. Landman; Phys. Rev. B41, 439 (1990); P. Stoltze, J. Norskov, and U. Landmann; Surf. Sci. 220, L693 (1989).
27. H. Dürr, R. Schneider and Th. Fauster; Vacuum 41, 376 (1990)
28. J.W.M. Frenken, F. Huussen and J.F. van der Veen; Phys. Rev. Lett. 58, 401 (1987)
29. C.S. Jayanthi, E. Tosatti, and L. Pietronero; Phys. Rev. B 31, 3456 (1985)
30. H.P. Bonzel and E. Latta; Surf. Sci. 76, 275 (1978)
31. H.P. Bonzel, in "Surface Mobilities on Solid Materials", Ed. Vu Thien Binh, (Plenum, New York, 1988), p. 195
32. H.P. Bonzel, N. Freyer, and E. Preuss; Phys. Rev. Lett. 57, 1024 (1986)
33. N. Freyer; Ph.D. thesis, Technische Hochschule Aachen (1985)

34. H.N. Yang, T.M. Lu, and G.C. Wang; Phys. Rev. Lett. 63, 1621 (1989) see also A. Pavlovska and E. Bauer; Appl. Phys. A 51, 172 (1990)
35. J.C. Heyraud and J.J. Metois; J. Cryst. Growth 82, 269 (1987)
36. G.A. Held, J.L. Jordan-Sweet, P.M. Horn, A. Mak, and R.J. Birgenau; Phys. Rev. Lett. 59, 2075 (1987)
37. S.M. Francis and N.V. Richardson; Phys. Rev. B 33, 662 (1986)
38. A.M. Lahee, J.P. Toennies, and Ch. Wöll; Surf. Sci. 191, 529 (1987); K.H. Rieder, private communication.
39. I.K. Robinson; private communication
40. J.C. Campuzano, M.S. Foster, G. Jennings, R.F. Willis and W. Unertl; Phys. Rev. Lett. 54, 2684 (1985)
41. P. Bak; Solid State Commun. 32, 581 (1979)
42. G. Binning, H. Rohrer, Ch. Gerber and E. Weibel; Surf. Sci. 131, L379 (1983)
43. J. Villain and I. Vilfan; Surf. Sci. 199, 165 (1988)
44. A.C. Levi and M. Touzani; Surf. Sci. 218, 223 (1989)
45. I.K. Robinson, E. Vlieg and K. Kern; Phys. Rev. Lett. 63, 2578 (1989)
46. K. Kern, I.K. Robinson, and E. Vlieg; Vacuum 41, 318 (1990)
47. T. Gritsch, D. Coulman, R.J. Behm and G. Ertl; Phys. Rev. Lett. 63, 1068 (1989)
48. J. Villain and I. Vilfan; Phys. Rev. Lett. 65, 1830 (1990)
49. M. den Nijs; this proceeding;
50. L.D. Roelofs, S.M. Foiles, M.S. Daw, and M. Baskes; Surf. Sci. 234, 63 (1990)
51. A.P. Baddorf and E.W. Plummer; J. Electr. Spectr. Related Phenom. 54,541 (1990)